Inorg. Chem. **2006**, *45*, 2397–2399

H_2, N_2, CO, and CO_2 Sorption Properties of a Series of Robust Sodalite-Type Microporous Coordination Polymers

Jorge A. R. Navarro,*,† Elisa Barea,† Juan M. Salas,† Norberto Masciocchi,*,‡ Simona Galli,‡ Angelo Sironi,§ Conchi O. Ania,|| and José B. Parra||

Departamento de Química Inorgánica, Universidad de Granada, Av. Fuentenueva S/N, 18071 Granada, Spain, Dipartimento di Scienze Chimiche e Ambientali, Università dell'Insubria, Via Valleggio 11, 22100 Como, Italy, Dipartimento di Chimica Strutturale e Stereochimica Inorganica, Università di Milano and ISTM-CNR, Via Venezian 21, 20133 Milano, Italy, and Department of Energy & Environment Instituto Nacional del Carbón, CSIC, Apartado 73, 33080 Oviedo, Spain

Received January 10, 2006

H_2, N_2, CO, and CO_2 are readily incorporated in the porous, 3D sodalitic frameworks of coordination polymers of the $[ML_2]_n$ type, with M = Pd^{II} or Cu^{II} and HL = 2-hydroxypyrimidine or 4-hydroxypyrimidine. The metal ion and ligand functionalization modulate their sorption properties, making these materials suitable for gas storage and separation purposes.

The optimization of the adsorption properties of porous solids is a present day challenge, boosted by industrial and environmental applications of selective gas storage, separation, and catalysis.[1,2] One of the most interesting classes of porous materials comprises the open metal−organic frameworks (MOFs).[3] These kinds of materials are extremely promising for H_2 storage applications and, although very high mass percent storage capacities (up to 3.8%) have been recently reported,[4] the usual low density of MOFs results in a low storage capacity on a volume basis, which should be subject to improvement by employing new synthetic strategies. Besides, the formation of MOFs involves a self-assembly process of metal fragments and organic spacers, which is facilitated by the use of labile metal ions [i.e., first-row, divalent transition-metal ions, Cu(I), Ag(I), Zn(II), and Cd(II)]. Pd(II) possesses an intermediate robustness, which makes it adequate for the obtention of stable discrete polynuclear systems with cavities and voids ready for molecular recognition and catalytic processes.[5] However, to the best of our knowledge, this metal ion has not yet been employed for the construction of crystalline porous coordination polymers.

We have recently reported the preparation, solid−liquid sorption, and structural properties of neutral and flexible 3D, sodalite-type coordination polymers of the $[CuL_2]_n$ formula, with L = 2-pyrimidinolate (2-pymo)[6] or 4-pyrimidinolate (4-pymo).[7] We have found that their overall structural features are nearly independent of the position of the exocyclic oxygen atom, but we have also shown that the shape, size, hydrophilicity, and ion-pair affinity of their cavities are highly affected.

In this Communication, we report the base-promoted polymerization of $[PdCl_2(2\text{-Hpymo})_2]$ (**1**), leading to a novel, 3D microporous sodalitic network, $[Pd(2\text{-pymo})_2]_n$ (**2**) (Figure 1), which is thermally stable up to 330 °C in air.[8] We also discuss the solid−gas adsorption properties of **2** and of its congeners, namely, $[Cu(2\text{-pymo})_2]_n$ (**3**)[6] and [Cu(4-

* To whom correspondence should be addressed. E-mail: jarn@ugr.es (J.A.R.N.), norberto.masciocchi@uninsubria.it (N.M.).
† Universidad de Granada.
‡ Università dell'Insubria.
§ Università di Milano and ISTM-CNR.
|| CSIC.

(1) For example, see: (a) Davis, M. M. E. *Nature* **2002**, *417*, 813. (b) Schlapbach, L.; Züttel, A. *Nature* **2001**, *414*, 353. (c) Fichtner, M. *Adv. Eng. Mater*. **2005**, *7*, 443.
(2) For example, see: (a) Lee, H.; Lee, J.; Kim, D. Y.; Park, J.; Seo, Y.; Zeng, H.; Moudrakovski, I. L.; Ratcliffe, C. I.; Ripmeester, J. A. *Nature* **2005**, *434*, 743. (b) Sozzani, P.; Bracco, S.; Comotti, A.; Ferretti, L.; Simonutti, R. *Angew. Chem., Int. Ed*. **2005**, *44*, 1816.
(3) For example, see: (a) Roswell, J. S.; Yaghi, O. M. *Angew. Chem., Int. Ed*. **2005**, *44*, 4670. (b) Kitagawa, S.; Uemura, K. *Chem. Soc. Rev*. **2005**, *34*, 109. (c) Ferey, G.; Mellot-Draznieks, C.; Serre, C.; Millange, F.; Dutour, J.; Surble, S.; Margiolaki, I. *Science* **2005**, *309*, 2040.
(4) (a) Ferey, G.; Latroche, M.; Serre, C.; Millange, F.; Loiseau, T.; Percheron-Guegon, A. *Chem. Commun.* **2003**, 2976. (b) Chen, B.; Ockwig, N. W.; Millward, A. R.; Contreras, D. S.; Yaghi, O. M. *Angew. Chem., Int. Ed*. **2005**, *44*, 4745.
(5) Fujita, M.; Tominaga, M.; Hori, A.; Therrien, B. *Acc. Chem. Res*. **2005**, *38*, 369.
(6) (a) Tabares, L. C.; Navarro, J. A. R.;. Salas, J. M. *J. Am. Chem. Soc*. **2001**, *123*, 383. (b) Barea, E.; Navarro, J. A. R..; Salas, J. M.; Masciocchi, N.; Galli, S.; Sironi, A. *J. Am. Chem. Soc*. **2004**, *126*, 3014.
(7) Barea, E.; Navarro, J. A. R.; Salas, J. M.; Masciocchi, N.; Galli, S.; Sironi, A. *Polyhedron* **2003**, *22*, 3051.
(8) Synthesis of **1**. An aqueous solution of K_2PdCl_4 (4 mmol) was mixed with another one containing 2-Hpymo·HCl (8 mmol). The suspension was stirred for 1 h, and a yellow microcrystalline powder was obtained. Yield: 95%. Calcd for $[Pd(C_4H_4N_2O)_2Cl_2]$: C, 26.05; H, 2.18; N, 15.16. Found: C, 26.17; H, 2.26; N, 15.39. Synthesis of **2**·H_2O. A water suspension of **1** (3 mmol in 50 mL of H_2O) was treated with a NaOH solution (1 M) until pH 6.0 was reached. The resulting suspension was refluxed for 5 days, affording a pale-yellow microcrystalline powder. Yield: 98%. Calcd for $[Pd(C_4H_3N_2O)_2]_n \cdot 3H_2O$: C, 27.41; H, 3.45; N, 15.98. Found: C, 27.78; H, 3.36; N, 15.53.

10.1021/ic060049r CCC: $33.50
Published on Web 02/24/2006

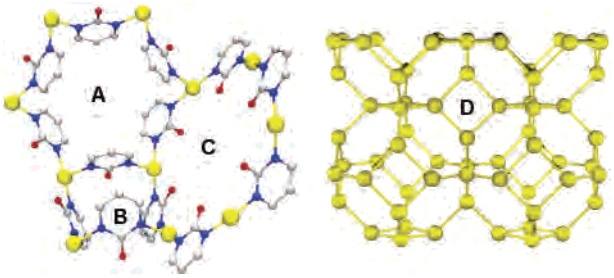

Figure 1. Structural motives found in the crystal structures of $[Pd(2\text{-}pymo)_2]_n{\cdot}2nH_2O$ (**2**·H_2O), $[Pd(2\text{-}pymo)_2]_n$ (**2**), and $[Cu(2\text{-}pymo)_2]_n$ (**3**): metallacalix[6]arene (A), metallacalix[4]arene (B), and planar molecular hexagon (C). Pd or Cu: yellow. O: red. N: blue. C: gray. D shows the zeotype sodalite framework found in materials **2**−**4**.

pymo)$_2]_n$ (**4**),[7] toward H_2, N_2, CO, and CO_2 in order to highlight the different roles of metal ions and pore stereochemistry in tuning the sorption properties.

The structural features of the precursor **1**, of the hydrated polymer $[Pd(2\text{-}pymo)_2]_n{\cdot}2nH_2O$ (**2**·H_2O), and of the anhydrous $[Pd(2\text{-}pymo)_2]_n$ form of the latter (**2**) have been disclosed by ab initio X-ray powder diffraction (XRPD) methods.[9] As expected, **1** consists of discrete square-planar *trans*-$[PdCl_2(2\text{-}Hpymo)_2]$ complexes (with N-monodentate 2-Hpymo ligands).

At variance, both **2**·H_2O and **2** are characterized by undistorted 3D, sodalite-type frameworks, built upon Pd(II) centers connected through N,N′-exobidentate 2-pymo bridges, which define three different structural motives, namely, planar molecular hexagons, metallacalix[4]arenes, and metallacalix[6]arenes (Figure 1). The three different structural motives interlock each other to build a 3D open framework of the sodalite zeotype (Figure 1D).

The local coordination of the Pd(II) ions is, as expected, square-planar, even in the hydrated phase **2**·H_2O, where the shortest Pd···O contacts fall well above 5.0 Å. At variance, short(er) "apical" bonds of the Cu···O type [2.76(3) Å] were observed in the hydrated **4**·H_2O phase, which results in a concomitant increase of ∼100 °C for the dehydration temperature.[7]

The porous framework of **2** is defined by the sodalitic β cages (Figure 1D), with an interior diameter of ca. 9 Å, interconnected by hexagonal windows. It should be noted that there are two kinds of hexagonal windows: one narrower (pore opening 4.8 Å) and hydrophilic (Figure 1C) and the other wider (8.8 Å) and hydrophobic (Figure 1A). Calculations with SMILE[10] show that, in the evacuated species **2**, the available volume for the inclusion is ca. 1800 Å^3 per unit cell, i.e. 42% of the crystal volume (see Table 1).

(9) Crystal data for **1**: $C_8H_8Cl_2N_4O_2Pd$, fw 369.49 g mol^{-1}, triclinic, $P\bar{1}$, a = 7.2254(3) Å, b = 8.5025(2) Å, c = 5.5925(2) Å, α = 97.876-(2)°, β = 110.901(2)°, γ = 109.065(2)°, V = 290.58(2) Å^3, Z = 1, ρ = 2.111 g cm^{-3}, T = 20 °C, R_{wp} = 0.143, R_p = 0.109, R_B = 0.040. Crystal data for **2**·H_2O: $C_8H_{10}N_4O_4Pd$, fw 332.61 g mol^{-1}, cubic, $Pn\bar{3}m$, a = 16.279(1) Å, V = 4315(1) Å^3, Z = 12, ρ = 1.536 g cm^{-3}, T = 20 °C; R_{wp} = 0.103, R_p = 0.077, R_B = 0.031. Crystal data for **2**: $C_8H_6N_4O_2Pd$, fw 296.58 g mol^{-1}, cubic, $Pn\bar{3}m$, a = 16.342(1) Å, V = 4364.0(8) Å^3, Z = 12, ρ = 1.354 g cm^{-3}, T = 130 °C, R_{wp} = 0.093, R_p = 0.073, R_B = 0.040. Data collected on a θ:θ Bruker D8 Advance diffractometer in the 5−105° range. CCDC Nos.: 275475−275477.

Table 1. Unit Cell and Pore Volumes for the Hydrated and Anhydrous Forms of **2**−**4**, BET Surfaces (m^2 g^{-1}; Calculated from the N_2 Adsorption Isotherms at 77 K), and Sorption Properties toward H_2 [Weight Percentage and Storage Density, $\rho_V(H_2)$, at 77 K and 900 Torr]

	cell volume; empty space; space group;% void		SA, m^2 g^{-1}	H_2, wt %	$\rho_V(H_2)$, kg L^{-1}
	RT hydrated	130 °C anhydrous			
2	4315; 1808; $Pn\bar{3}m$; 41.9	4364; 1801; $Pn\bar{3}m$; 41.3	600	1.29	0.018
3	3852; 1257 (3×); $R\bar{3}m$; 32.6	3422; 953; $Pn\bar{3}m$; 27.8	350	0.86	0.013
4	3910; 1240; $P4_232$;[a] 31.7	3512; 1033; $P4_232$;[a] 24.4	65	0.03	0.0004

[a] Idealized ordered model.

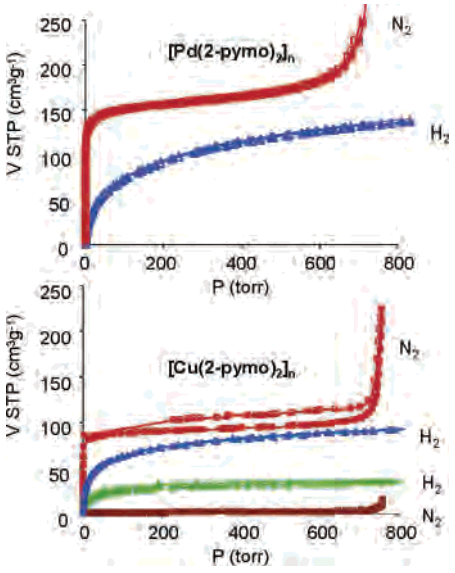

Figure 2. Isotherms at 77 K for the adsorption of H_2 [triangles; activation temperature (blue) 120 °C, (green) 105 °C] and N_2 [squares; activation temperature (red) 120 °C, (brown) 105 °C] on **2** (top) and **3** (bottom). Desorption is denoted by open symbols.

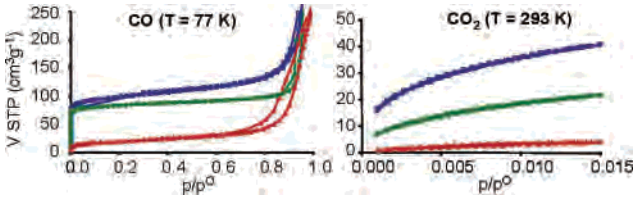

Figure 3. CO and CO_2 adsorption isotherms for **2** (blue squares), **3** (green circles), and **4** (red triangles). Desorption is denoted by open symbols.

To evaluate the permanent porosity of the open frameworks **2**−**4** and to estimate their possible use in catalysis and for gas separation or storage application purposes, we have studied the sorption isotherms of H_2, N_2, and CO at 77 K and of CO_2 at 293 K (see Figures 2 and 3).[11] The N_2 and CO isotherms are of type I and reversible in all cases, except **3** (see note ref 12 and Table 1), indicative of materials with pores in the nanometer range. Indeed, density functional theory (DFT)[13] and Horvath−Kawazoe analysis[14] of the N_2 isotherms for **2** and **3** account for adsorption taking place in very narrow pores (<11 Å width), in agreement with the

(10) Eufri, D.; Sironi, A. *J. Mol. Graphics* **1989**, *7*, 165.
(11) Isotherms have been measured volumetrically (Micromeritics 2010 M equipment) on degasified samples at 120 °C and under vacuum for 12 h.

values obtained for the sodalitic β cages by our crystal structure analysis (ca. 9 Å; see above). The results are also in agreement with strong adsorbate−adsorbent interactions, with the micropores being filled by N_2 and CO guest molecules at very low pressures. In addition, **2** and **3** show a relatively high capacity for CO_2 storage, viz. ca. 3 and 1.5 CO_2 molecules per β cage,[15] respectively, at room temperature and low relative pressures (Figure 3).

2 and **3** also show fully reversible type I H_2 sorption isotherms, indicative of the filling of the micropores only. It is worth noting that the two species possess a relevant capacity of H_2 storage at 77 K and 900 Torr: ca. 1.3% and 0.86% weight percentage, i.e., 11.6 and 6.6 H_2 molecules per β cage, respectively. This results in high storage volumetric densities, viz., 0.018 kg of H_2/L for **2** and 0.013 kg of H_2/L for **3**. Thus, **2** overcomes the highest known values observed for MOF-type materials *at similar* experimental conditions, namely, 0.017 kg of H_2/L for MOF-505 [Cu_2(bptc)],[4b] which shows the maximum known value of H_2 weight percentage uptake (2.47% at 77 K and 760 Torr). Another implication of the gas sorption performances of **2** and **3** is the relative surface coverage of H_2 molecules[16] (83 and 94%, respectively), which are among the highest known values, i.e., $Mn(HCOO)_2$ (150%),[17] $Cu_3[Co(CN)_6]_2$ (94%),[18] [Cu_2(bptc)] (52%),[4b] zeolite HSSZ-13[19] (76%), and highly activated porous carbon materials (38%).[1b] The steep slope of the hydrogen sorption isotherms of **2** and **3** in the low-pressure range is also indicative of the strong interaction of the hydrogen molecules with the pore walls. It is noteworthy that **2**, based on the heavier Pd, outperforms the behavior of **3** and **4**, thanks to the significantly longer M−N bonds in **2**, leading to a higher pore surface (see below and Table 1). It is also interesting to note that the much steeper slope of the N_2/CO isotherms than the H_2 ones in the low-pressure range clearly points to a N_2/CO selectivity of **2** and **3** over H_2.

In addition, it should be noted that **3** and **4**, although sharing nearly equal cell parameters and empty volumes, have different sorption performances. Indeed, they mainly differ in the distinct decoration of the metallacalix[6]arene motives: in **3**, the internal surface of these pores is covered by hydrogen atoms, while some of them (one out of three) are substituted by oxygen atoms in **4**. Presumably, the oxygen atoms in **4**, pointing away from the Cu atoms into the open cavities, hinder the diffusion of adsorbate molecules through the pores, thus accounting for the dramatic lowering of its affinity for guest molecules.

Another interesting feature of **3** is the marked effect of the activation temperature on its adsorption selectivity. Thus, activation at 105 °C results in no measurable N_2 uptake and significant, although slow, sorption of H_2 (0.33 wt %) (Figure 2). This effect can be explained by the presence of a few residual water molecules in the host MOF, hindering the diffusion of large guests (N_2) but allowing smaller molecules (like H_2) to permeate.

From the analysis of the unit cell volumes of the hydrated and anhydrous species (see Table 1), a structural interpretation of the sorption behavior can be derived. Indeed, (i) given the actual site symmetry of the metal ions, the size of the unit cell *strictly* depends on the M−N bond distances, which control the X-pymo-bridged M···M contacts (i.e., the edges of the sodalitic framework): longer M−N values [e.g., for Pd(II)] thus *cooperatively* result in a much larger empty volume and higher surface area (as observed in **2**); (ii) the copper species **3** and **4** (reversibly) deflate (by as much as 430 Å^3 per unit cell, or 11%) to their evacuated analogues upon loss of water molecules because Cu−N bonds shrink with the lowering of the Cu(II) coordination number in the anhydrous phase;[7] (iii) such an effect is not observed on passing from **2**·H_2O to **2**, probably because the low tendency of Pd(II) ions to coordination numbers higher than 4 forces the water molecules to cluster in the sodalitic cages.[20]

As far as the sorption of hydrogen is concerned, the performance of **2** closely approaches those of the best MOFs reported up to date[3a,4] on a volume basis. This is related to the empty volume actually available for inclusion and to the stability of the framework.

In light of possible practical applications, another remarkable feature of **2** and **3** is the reversibility of their sorption isotherms; moreover, their ability for adsorption of molecules other than H_2 (i.e., H_2O, CO, and CO_2) should also be emphasized because the removal of small amounts of contaminant gases from H_2 is still an open challenge for the real use of hydrogen as a fuel.[21]

Acknowledgment. Support by the Spanish and Italian Ministries of Science (Grants CTQ2005-00329/BQU, EX2004-0612, and HI2003-0081).

Supporting Information Available: XRPD and thermodiffractometric results, thermogravimetry, and sorption isotherms. This material is available free of charge via the Internet at http://pubs.acs.org.

IC060049R

(12) The irreversibility of the N_2 isotherm for **3** in the microporous region can be related to a probable structural phase change taking place upon guest uptake.[6] On the other hand, the N_2 and CO isotherms of **2**−**4** show interparticle gas condensation at pressures close to the saturation point, which should be related to the small particle size (a few hundred angstroms) of these microcrystalline materials.

(13) DFT analyses have been performed using a Micromeritics metal oxide model of cylindrical pores.

(14) Horvath, G.; Kawazoe, K. *J. Chem. Eng. Jpn.* **1983**, *16*, 470.

(15) There are two symmetry-equivalent β cages in the unit cell.

(16) The relative surface coverage can be calculated by assuming that the monolayer condensation of hydrogen on a solid surface leads to a maximum of 1.3×10^{-5} mol m^{-2} of adsorbed hydrogen.[1b]

(17) Dybtsev, D. N.; Chun, H.; Yoon, S. H.; Kim, D.; Kim, K. *J. Am. Chem. Soc.* **2004**, *126*, 32.
(18) Kaye, S. S.; Long, J. R. *J. Am. Chem. Soc.* **2005**, *127*, 6506.
(19) Zecchina, A.; Bordiga, S.; Vitillo, J. G.; Ricchiardi, G.; Lamberti, C.; Spoto, G.; Bjørgen, M.; Lillerud, K. P. *J. Am. Chem. Soc.* **2005**, *127*, 6361.

(20) Thermodiffractometry in the 25−130 °C range showed a very small cell volume decrease below 50 °C, followed by a linear, but very limited, increase, given by thermal expansion only. This process was found to be completely reversible. No structural change is observed up to ca. 330 °C, where the sample, heated in air, begins to decompose.

(21) Atwood, J. L.; Barbour, L. J.; Jerga, A. *Angew. Chem., Int. Ed.* **2004**, *43*, 2948.